11th Australasian Fluid Mechanics Conference
University of Tasmania, Hobart, Australia
14-18 December 1992

FLUID DYNAMICS, HEAT TRANSFER AND SOLIDIFICATION IN STRIP-CASTING METAL-DELIVERY SYSTEMS

J.S. TRUELOVE[1], T.A. GRAY[2] and P.C. CAMPBELL[1]

[1]BHP Research, Newcastle Laboratories, PO Box 188, Wallsend, NSW 2287, AUSTRALIA

[2]Dept of Petroleum Engineering, University of New South Wales, Kensington, NSW 2033, AUSTRALIA

ABSTRACT

A theoretical and experimental investigation of fluid flow, heat transfer and solidification in a high-speed strip-casting metal-delivery system is presented. The theoretical formulation is based on the time-averaged equations for conservation of mass, momentum and energy supplemented by a two-equation turbulence model and phenomenological models to describe the flow and latent heat release in the mushy, phase-change zone. Experimental results from full-scale water models are used to evaluate the flow predictions of the theoretical model. The theoretical model is applied to examine the effects of geometry and thermal conditions on liquid metal flow and shell growth, and key operating parameters are identified. Solidification on the moving substrate is shown to have a significant effect on the flow pattern within an extended pool. Shell growth is shown to be controlled by the resistance to heat transfer between the steel and the cooled substrate.

INTRODUCTION

Numerous metal-delivery systems have been proposed for continuous casting of thin steel strip. In the planar-flow approach, liquid steel is delivered onto a moving cooled substrate through a narrow nozzle of fixed and controlled dimensions. A schematic diagram of a belt caster is shown in Fig. 1.

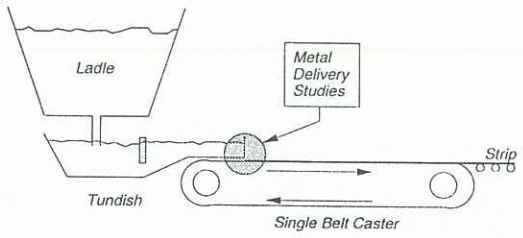

Fig. 1 Schematic of a belt caster.

The basic component of the planar-flow caster is the liquid-delivery nozzle. Two nozzle configurations are shown schematically in Fig. 2. In each configuration, liquid steel from an elevated tundish is delivered under gravity over a back wall while partially solidified steel is withdrawn through a narrow gap between the front wall and the moving belt. The extended-pool delivery system shown in Fig. 2b is designed to enhance shell growth by increasing the length of contact between molten steel and cooled substrate while under the pressure provided by the ferro-static head of the pool within the nozzle enclosure.

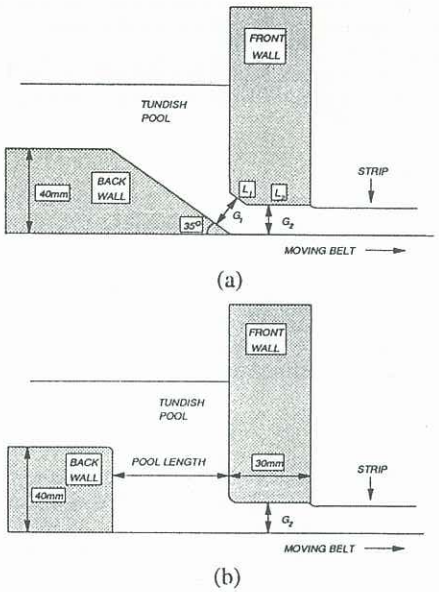

Fig. 2 Schematic of metal delivery nozzles: (a) slot nozzle; (b) extended-pool nozzle.

The quality of the strip produced is governed by two key factors: liquid flow to the substrate and solidification on the substrate. The design requirements for a thin-strip caster demand relatively high casting speeds, typically around 1m/s for 6mm strip. Consequently, the flow adjacent to the moving belt and within the nozzle is turbulent. Solidification of alloys such as steel occurs over a temperature range, from liquidus to solidus of typically 50°C, and is accompanied by the formation of closely spaced 'tree-like' structures, called columnar dendrites, that grow from the solid shell into the liquid and form what is known as a mushy zone. Although considerable progress has been made in understanding flow and heat transfer during solidification processes (Salcudean and Abdullah, 1988), little attention has been given to elucidating the complex effect of turbulence on the flow of interdendritic liquid, which has important implications for heat transfer and shell growth.

The purpose of this paper is to develop a mathematical model of the thin-strip caster and apply the model to identify key operating parameters. Attention is focussed on the effects of pool geometry, melt superheat and steel-substrate heat transfer on the flow distribution in the liquid and the shell growth at the substrate. The model predictions for the flow distribution in the absence of solidification are evaluated by comparison with data from full-scale water-modelling trials.

MODEL FORMULATION

The mathematical model is based on the time-averaged equations for conservation of mass, momentum and energy, supplemented by the $k-\varepsilon$ turbulence model and phenomenological models to describe the flow and latent heat release in the mushy, phase-change zone.

Fluid-Flow Equations

The modelling of fluid flow during solidification of liquid metals has to account for a solidified region, a liquid region and a mushy zone between the solid and liquid regions. For the purpose of model formulation it is expedient to consider the whole of the flow domain as a porous medium, with porosity one in the liquid, zero in the solid, and intermediate between one and zero in the mushy zone.

According to Darcy's law, the velocity of liquid flowing through a porous medium is proportional to the pressure gradient. This relationship is embodied in the momentum equation by the addition of a source term proportional to the velocity. Physically this extra source term represents the drag due to liquid-metal flow in the mushy zone.

The generalised time-averaged equations for conservation of mass and momentum, applicable throughout the flow domain in the liquid, mushy and solid regions, are (Bennon and Incropera, 1987):

$$\nabla \cdot (\rho \mathbf{U}) = 0 \tag{1}$$

$$\nabla \cdot (\rho \mathbf{U}\mathbf{U}) = -\nabla P + \nabla \cdot (\mu_e \mathbf{D}) + \rho \mathbf{g} - A(\mathbf{U} - \mathbf{U}_s) \tag{2}$$

where ρ is the density, P the pressure, $\mathbf{g}$ the gravitational acceleration, μ_e the effective viscosity, and $\mathbf{D}$ the deformation tensor. $\mathbf{U}$ is the superficial velocity for the liquid-solid system defined by:

$$\mathbf{U} = \theta \mathbf{U}_l + (1-\theta)\mathbf{U}_s \tag{3}$$

where $\mathbf{U}_l$ and $\mathbf{U}_s$ are the interstitial liquid and solid substrate velocities respectively, and θ is the liquid volume fraction, or porosity.

The functional form for A is chosen to ensure the correct asymptotic behaviour for the momentum equation: in the liquid, A is zero and the Darcy source vanishes; and in the solid, A is large and the superficial velocity is equal to the casting velocity. In this work the functional form of the Carman-Kozeny equation is adopted:

$$A = C\frac{(1-\theta)^2}{\theta^3} \tag{4}$$

where C is a constant dependent on the liquid viscosity and the characteristic dimensions and morphology of the dendritic array. In this study C is set to 10^9 kg/m^3.s, based on correlations of experimental data by Poirier (1987) and measurements of dendrite arm spacing in strip-cast steel.

Turbulence Equations

Turbulence is represented by a generalised form of the well-established $k-\varepsilon$ model. Within the mushy zone, the closely spaced dendrites act to rapidly damp turbulent fluctuations. To model this dissipation process, a sink term is added to the k equation. Consideration of the Darcy source term added to the momentum equation to represent drag leads to an added source term $-Ak$ in the k equation. To maintain internal consistency in the two-equation turbulence model additional terms are required in the ε equation. Again, consideration of the Darcy term leads to an added source $-2A\varepsilon - 2\nu\nabla A \cdot \nabla k$. Here, the second term is large and positive within the mushy zone and serves to rapidly damp the turbulence energy. Physically, this term accounts for the decrease in length scale characteristic of the flow within the mushy zone.

The modelled equations for k and ε used in this work are:

$$\nabla \cdot (\rho \mathbf{U}k) = \nabla \cdot (\mu_e \nabla k) + G_k - \rho\varepsilon - Ak \tag{5}$$

$$\nabla \cdot (\rho \mathbf{U}\varepsilon) = \nabla \cdot (\mu_e \nabla \varepsilon) + (C_1 G_k - C_2 \rho\varepsilon)\,\varepsilon/k - 2A\varepsilon - 2\nu\nabla A \cdot \nabla k \tag{6}$$

These equations provide a plausible description of the turbulence throughout the flow domain: in the liquid, the equations reduce to the standard $k-\varepsilon$ model; in the solid, k vanishes; and in the mushy zone k is damped rapidly with decreasing liquid fraction.

Energy Equation

It is convenient to introduce the total system enthalpy defined as:

$$H = \int C_p dT + \theta L \tag{7}$$

where the first term represents the sensible heat, and the second the latent heat with L the latent heat of fusion.

When energy transfer is predominantly by convection and diffusion, with negligible radiation, then the energy equation may be written in terms of H as (Voller and Prakash, 1987):

$$\nabla \cdot (\rho \mathbf{U}H) = \nabla \cdot (k_e \nabla T) - \nabla \cdot [\rho(\mathbf{U} - \mathbf{U}_s)(1-\theta)L] \tag{8}$$

where k_e is the effective thermal conductivity, given by the sum of the molecular conductivity and the turbulent conductivity derived from the turbulent viscosity. The second term on the right hand side represents a correction to convective transport of enthalpy arising from the assumption that solidifying steel in the mushy zone consists of dendrites moving with the substrate velocity and not the system velocity. The correction term vanishes in the liquid and solid. The energy equation is applicable throughout the flow domain.

The liquid fraction is associated with the latent heat content in the mushy zone and varies from zero to one through the zone. When latent heat is assumed to be released uniformly in the mushy zone then the liquid fraction can be expressed in terms of the total enthalpy and the enthalpies at the solidus and liquidus temperatures.

Boundary Conditions

The velocity, turbulence and temperature at the inlet are prescribed. At the free surface and outlet, zero-normal-gradient conditions are imposed for streamwise velocity, turbulence and enthalpy. At solid surfaces, so-called wall functions are used to bridge the boundary layer; the no-slip condition is imposed for velocity and prescribed heat-flux conditions for enthalpy. At the substrate surface, the heat flux is expressed in terms of an overall steel-substrate heat-transfer coefficient. At surfaces adjacent to solidified steel, the boundary conditions for velocity and turbulence are effectively imposed by the added source terms in the transport equations, while the condition for enthalpy reduces to a balance between conduction in the solidified steel and the substrate.

Method of Solution

The governing equations are expressed in a two-dimensional Cartesian coordinate system, reduced to a conservative finite-difference form using the control-volume method, and solved by well-established computational techniques. Under-relaxation is employed to avoid instability arising from the strong coupling between the momentum and energy equations.

WATER FLOW EVALUATION

Measurements in a full-scale (150mm wide) water model of the tundish and metal-delivery system were obtained for model evaluation. Both Reynolds and Froude number similarity are achieved by the model, providing a direct

comparison between water and steel flows when the effects of solidification are ignored.

Figure 3 compares predicted and measured flowrate-head relations for three gap settings of the slot nozzle shown in Fig. 2a. Both predictions and measurements indicate that the flowrate is primarily controlled by the gap G_2 between the nozzle and the belt, with a secondary influence of the gap G_1 in the nozzle approaching the belt. The gap lengths (20-40mm) and belt speed (0-1m/s) have no appreciable effect on the flowrate through the slot nozzle.

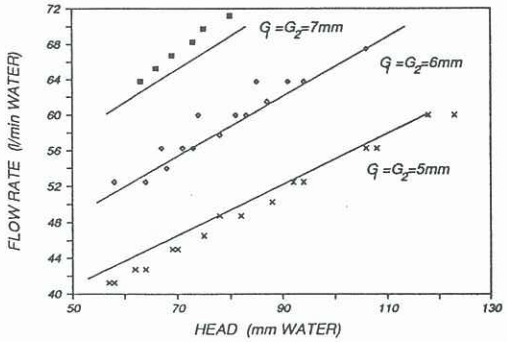

Fig. 3 Water flowrate as a function of head.

The flowrate through the extended-pool nozzle shown in Fig. 2b is again primarily controlled by the gap between the front wall and the belt. In the case of the extended pool, however, the head increases or decreases slightly with increasing contact length depending on whether the belt is stationary or moving. The stationary belt produces a drag which increases the head required to provide a given flowrate; conversely, the moving belt supplies a 'pumping action' which decreases the required head. The head is essentially independent of the back-wall geometry. The trends predicted for the stationary belt are confirmed by the measurements.

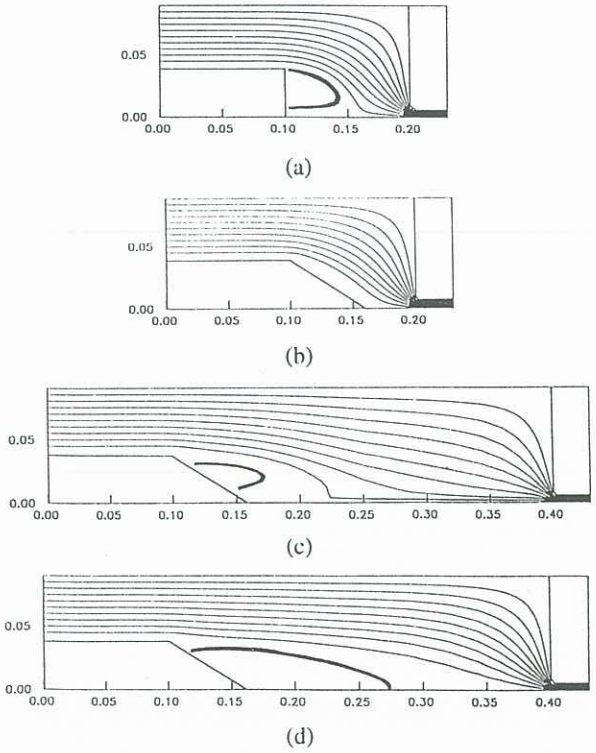

Fig. 4 Water flow patterns: (a)-(c) moving belt; (d) stationary belt.

Figure 4 shows the predicted flow patterns (streamlines) in the extended-pool nozzle for a range of cases chosen to illustrate the influence of the three major variables under consideration: pool length, back-wall geometry and belt movement. Of particular concern is the occurrence of recirculation within the pool immediately behind the back wall. In a metal-delivery system, recirculation is undesirable due to the likelihood of meniscus instability and freezing. The zone of recirculation is shown by the bold streamline.

Within the range of conditions examined, the length of the recirculation zone increases with increasing pool length. A sloping back wall decreases the zone of recirculation. As shown in Figs. 4a and 4b, the sloping wall eliminates recirculation altogether for short pool lengths. A moving belt significantly reduces the zone of recirculation. As shown in Fig. 4c, the streamlines deflect toward the belt as a consequence of flow induced by the drag of the moving surface, enhancing 'contact' between the fluid and the belt and reducing the tendency evident in Fig. 4d for the bulk of the fluid to flow directly from the tundish to the nozzle 'bypassing' the substrate.

Measurements of recirculation length for the case of a stationary belt were obtained by visual observation of a stream of dye introduced into the flow near the reattachment point. The predicted and measured trends are in very good agreement.

STEEL SOLIDIFICATION PREDICTION

Predictions of caster performance with the extended-pool delivery system have been obtained for a casting rate of 1m/s, melt superheats ΔT of 10°C and 50°C, and steel-substrate heat-transfer coefficients h_s of 5 and 10kW/m^2.K. Typical thermophysical properties are used for the steel: in particular, the kinematic viscosity is the same as that for water and the difference between the liquidus and solidus temperatures is taken as 50°C.

Figure 5 shows the calculated head as a function of contact length for the liquid metal and water flows. The comparison suggests that the head for the steel flow is significantly lower than the corresponding head for the water flow, due to the enhanced coupling between the moving substrate and the liquid provided by the mushy zone.

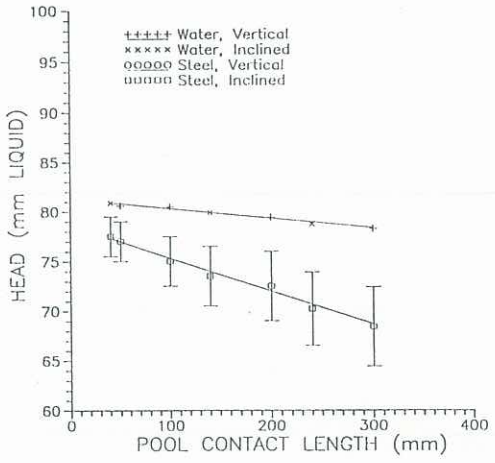

Fig. 5 Head as a function of contact length for water and steel. Error bars indicate variation with ΔT and h_s.

The variations in head with melt superheat and steel-substrate heat-transfer coefficient exhibit no clear trend and the predictions suggest a rather complex behaviour. In general, the head is expected to correlate with the width of the mushy zone; a narrow mushy zone resulting in a high head approaching that for water, and a wide mushy zone resulting in a low head due to the enhanced 'pumping action' referred to above. The width of the mushy zone is

influenced by steel properties and caster operating conditions; in particular, the little-understood effect of turbulence on the flow of interdendritic liquid might be expected to play a significant role.

Figure 6 shows the predicted steel flow patterns corresponding to the first three water flow configurations in Fig. 4, from which it can be seen that the zones of recirculation are remarkably similar for steel and water.

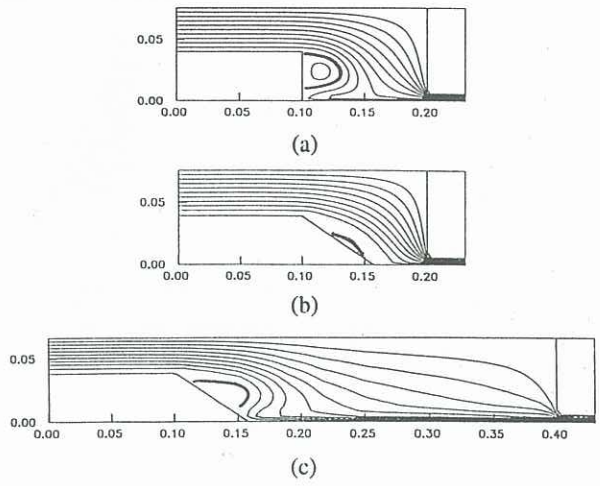

Fig. 6 Steel flow patterns for ΔT=10°C, h_s=10kW/m^2.K.

Solidification has an important effect on the flow streamlines: the flow of liquid toward the moving substrate, observed in the case of water flows, is greatly enhanced by solidification as evidenced by the strong deflection of streamlines toward the substrate. Thus, solidification within the pool further enhances 'contact' between the liquid steel and the substrate, reducing the tendency for fluid to 'bypass' the substrate.

Figure 7 shows the effect of steel-substrate heat-transfer coefficient on the flow prediction. The streamline patterns are qualitatively similar and suggest that the flow is relatively insensitive to thermal conditions within the range of parameters examined.

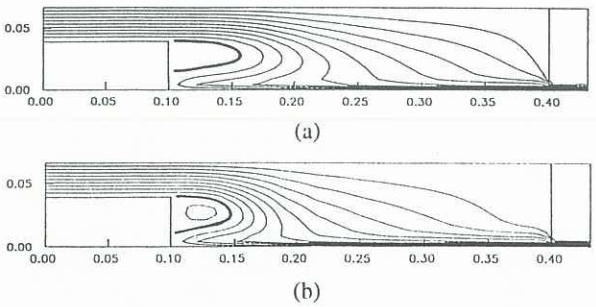

Fig. 7 Steel flow patterns for ΔT=10°C: (a) h_s=10kW/m^2.K; (b) h_s=5kW/m^2.K.

There are, however, some detailed differences in the flow streamlines approaching the front wall: for the flow with the lower value of h_s the stagnant region near the free surface is enlarged and on the verge of recirculating. The onset of recirculation at the front wall is a consequence of the relatively high streamwise velocities in the fluid immediately upstream of the narrow nozzle gap. Recirculation adjacent to the front wall is also undesirable due to the likelihood of freezing.

Figure 8 shows the predicted shell thickness as a function of the substrate contact length for various melt superheats and steel-substrate heat-transfer coefficients. The thickness of solidified steel at the nozzle exit is of major practical concern to the operation of the metal-delivery system.

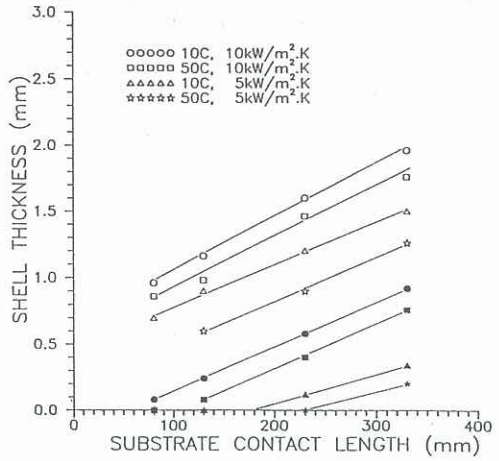

Fig. 8 Shell thickness as a function of contact length.

As can be seen, the thickness of solidified steel, indicated by the solidus contour, increases approximately linearly with substrate contact length for the range of conditions examined. As expected, the steel-substrate heat-transfer coefficient controls the rate of increase in the thickness of solidified steel, while the melt superheat determines the distance to the onset of solidification. Conduction through the solidified shell has little influence on the rate of shell growth for very thin strip. After the onset of solidification, the width of the mushy zone, between the liquidus and solidus contours, is essentially constant for the rather limited range of contact lengths considered.

CONCLUSIONS

The following main practical conclusions can be drawn from the present investigation.

- Flow through the liquid-delivery nozzle is controlled by the head of liquid and the dimension of the narrow gap between the front wall and the substrate.
- The predicted flow patterns for water and steel are qualitatively similar. Substrate motion in an extended-pool delivery system enhances 'contact' between the fluid and the substrate and reduces the tendency for the bulk fluid to flow directly from the tundish to the nozzle, 'bypassing' the substrate. The influence of substrate motion is enhanced by solidification.
- The rate of increase in the thickness of solidified steel is controlled by the resistance to heat transfer between the steel and the cooled substrate, while the melt superheat governs the distance to the onset of solidification.
- Experimental work is needed to evaluate the predictions for the steel flows and validate the model developed to represent turbulence effects within the mushy zone.

REFERENCES

BENNON, W D and INCROPERA, F P (1987) The evolution of macrosegregation in statically cast binary ingots, Met. Trans. B., 18B, 611-616.

POIRIER, D R (1987) Permeability for flow of interdendritic liquid in columnar-dendritic alloys, Met. Trans. B., 18B, 245-255.

SALCUDEAN, M and ABDULLAH, Z (1988) On the numerical modelling of heat transfer during solidification processes, Int. J. Numerical Methods in Engineering, 25, 445-473.

VOLLER, V R and PRAKASH, C (1987) A fixed grid numerical modelling methodology for convection-diffusion mushy region phase-change problems, Int. J. Heat Mass Transfer, 30, 1709-1719.